ATP Acts as a Regulatory Effector in Modulating Structural Transitions of Cytochrome *c*: Implications for Apoptotic Activity[†]

Antonella Patriarca,[‡] Tommaso Eliseo,[§] Federica Sinibaldi,[‡] Maria Cristina Piro,[‡] Riccardo Melis,[§] Maurizio Paci,[§] Daniel O. Cicero,[§] Fabio Polticelli,[||] Roberto Santucci,[‡] and Laura Fiorucci*[,‡]

Department of Experimental Medicine and Biochemical Sciences and Chemical Science and Technology, University of Rome "Tor Vergata", 00133 Rome, Italy, and Department of Biology, University "Roma Tre", 00146 Rome, Italy

Received September 29, 2008; Revised Manuscript Received February 19, 2009

ABSTRACT: The binding of lipids (free fatty acids as well as acidic phospholipids) to cytochrome *c* (cyt *c*) induces conformational changes and partial unfolding of the protein, strongly influencing cyt *c* oxidase/peroxidase activity. ATP is unique among the nucleotides in being able to turn non-native states of cyt *c* back to the native conformation. The peroxidase activity acquired by lipid-bound cyt *c* turns out to be very critical in the early stages of apoptosis. Nucleotide specificity is observed for apoptosome formation and caspase activation, the cleavage occurring only in the presence of dATP or ATP. In this study, we demonstrate the connection between peroxidase activity and oleic acid-induced conformational transitions of cyt *c* and show how ATP is capable of modulating such interplay. By NMR measurement, we have demonstrated that ATP interacts with a site (S1) formed by K88, R91, and E62 and such interaction was weakened by mutation of E62, suggesting the selective role in the interaction played by the base moiety. Interestingly, the interactions of ATP and GTP with cyt *c* are significantly different at low nucleotide concentrations, with GTP being less effective in perturbing the S1 site and in eliciting apoptotic activity. To gain insights into the structural features of cyt *c* required for its pro-apoptotic activity and to demonstrate a regulatory role for ATP (compared to the effect of GTP), we have performed experiments on cell lysates by using cyt *c* proteins mutated on amino acid residues that, as suggested by NMR measurements, belong to S1. Thus, we provide evidence that ATP acts as an allosteric effector, regulating structural transitions among different conformations and different oxidation states of cyt *c*, which are endowed with apoptotic activity or not. On this basis, we suggest a previously unrecognized role for ATP binding to cyt *c* at low millimolar concentrations in the cytosol, beyond the known regulatory role during the oxidative phosphorylation in mitochondria.

Cytochrome *c* (cyt *c*)[1] is a heme-protein bound on the external side of the inner mitochondrial membrane via the interaction with the phospholipid cardiolipin (CL). There, it functions as a mobile electron carrier in the respiratory chain shuttling electrons from cyt *c* reductase to cyt *c* oxidase. ATP binds to cyt *c* and can modulate the rate of electron exchange with its redox partners (*1*), inducing changes in its oxidation state. In the native cyt *c*, H18 and M80 are the axial ligands of the hexacoordinated low-spin heme iron. The binding of lipids (free fatty acids as well as acidic phospholipids) to cyt *c* directly affects the sixth coordination position of the heme iron by displacement of M80 (*2*−*5*), strongly influencing cyt *c* oxidase/peroxidase activity (*6, 7*). In the phospholipid−cyt *c* interaction model, one phospholipid chain is accommodated in a hydrophobic channel present in the protein structure (*2*). The entry point for acyl chain insertion is not known; however, the most frequently identified residues in the binding surface of the CL−cyt *c* complex are K72, K73, K86, K87, and R91 (*8*−*11*). Importantly, the peroxidase activity acquired by CL-bound cyt *c* turns out to be very critical in the early stages of apoptosis; it generates CL selective peroxidation, an event that precedes release of cyt *c* from mitochondria during apoptosis (*6, 7, 12*).

Release of cyt *c* from the inner mitochondrial membrane into the cytosol in response to specific signals is considered the point of no return in cell death. In the cytosol, cyt *c* binds to Apaf-1, inducing, in the presence of ATP or dATP, the formation of Apaf-1 multimers and the recruitment of procaspase-9 (*13*). Repeated observations have revealed that oxidized cyt *c* is able to induce caspase activation in the cytosol, whereas reduced cyt *c* has little or no capacity to activate the caspases most likely because the reduced and oxidized forms of cyt *c* have different binding affinities for

[†] Research funded in part by grants from Italian MIUR (PRIN 2007KAWXCL).

* To whom correspondence should be addressed: Department of Experimental Medicine and Biochemical Sciences, University of Rome "Tor Vergata", via Montpellier 1, 00133 Rome, Italy. Telephone: 39-06-72596478. Fax: 39-06-72596477. E-mail: fiorucci@uniroma2.it.

[‡] Department of Experimental Medicine and Biochemical Sciences.

[§] Chemical Science and Technology, University of Rome "Tor Vergata".

[||] University "Roma Tre".

[1] Abbreviations: cyt *c*, horse heart cytochrome *c*; CL, cardiolipin; Apaf-1, apoptotic protease-activating factor 1; NMR, nuclear magnetic resonance; CD, circular dichroism; GdnHCl, guanidine hydrochloride; DTT, 1,4-dithiothreitol; Ac-DEVD-AMC, acetyl-Asp-Glu-Val-Asp-7-amino-4-methylcoumarin; Ac-LEHD-AFC, acetyl-Leu-Glu-His-Asp-7-amino-4-trifluoromethylcoumarin; GSH, glutathione.

10.1021/bi801837e CCC: $40.75
Published on Web 02/20/2009

Apaf-1 (*14*−*16*). Binding of cyt *c* to Apaf-1 involves several lysine residues located in different areas of the protein surface, particularly K7, K25, K39, and K72, all surrounding the heme edge and interacting with the negatively charged aspartate residues in the Apaf-1 WD-40 domain (*17, 18*).

A previous work has shown that fatty acid binding to cyt *c* induces a folding variant with the typical features of a molten globule state and that ATP is able to return that conformation to its native one (*19*). Our study suggests a physiological role for ATP binding to cyt *c* at low millimolar concentrations in the cytosol, beyond the regulatory role previously reported in the oxidative phosphorylation in mitochondria (*1*). On the basis of the results obtained, here we propose that ATP acts as an allosteric effector, regulating structural transitions among different conformations of cyt *c*, which are endowed with apoptotic activity or not. Hence, the structural features of cyt *c* required for its pro-apoptotic activity have been investigated by performing mutations on amino acid residues that, as suggested by NMR measurements, belong to a specific ATP binding site on cyt *c*.

EXPERIMENTAL PROCEDURES

Construction of the Horse cyt c Expression System and Mutants. A version of the h-cyt *c* synthetic gene was designed on the basis of the sequence of a previously reported cyt *c* synthetic gene (*20*) and its synthesis accomplished by Primm srl (Milan, Italy). We converted the pBTRI plasmid to the horse cyt *c* expression plasmid by removing the yeast iso-1-cyt *c* gene and replacing it with the new synthetic h-cyt *c* gene. The sequence of the expression construct (pHCyc) was confirmed by the DNA sequence (M-Medical, Milan, Italy). The pHCyc plasmid was then subjected to one round of mutagenesis, which introduced the single E62N, K88E, or R91N substitution into the h-cyt *c* gene. Production of the double mutant K88E/E62N was achieved from the single mutant pHCyc-K88E plasmid, which was used as the template in a second round of mutagenesis. All mutants and wt h-cyt *c* expression plasmids were introduced into *Escherichia coli* strain JM 109, and bacterial expression and purification of the recombinant proteins were conducted as previously described (*21*). Uniformly ^{15}N-labeled horse heart cyt *c* and the E62N mutant were isolated from cultures created in M9 minimal medium containing 1.0 g/L $^{15}NH_4Cl$, supplemented with a solution of trace elements, a vitamin mix, and the appropriate antibiotics. Expression and purification of recombinant proteins were conducted as described above.

Electronic Absorption. Absorption measurements were carried out at 25 °C using a Cary 5 spectrophotometer. The ferric cyt *c* concentration was determined on the basis of an extinction coefficient ε of 106 mM^{-1} cm^{-1} at 408 nm. The redox status of cyt *c* was determined by monitoring the absorbance at 550 nm (A_{550}).

Circular Dichroism Spectroscopy. CD spectra in the far-UV (200−250 nm) and Soret (400−450 nm) regions were recorded on a Jasco-710 spectropolarimeter (Jasco, Tokyo, Japan) equipped with a personal computer as a data processor and a temperature-controlled holder maintained at 25 °C. Quartz cells with 1 and 5 mm light paths were used for measurements in the far-UV and Soret regions, respectively. Spectra were obtained for samples containing 7 μM cyt *c* (in ferric form, wt, and mutants) in the absence and presence of different concentrations (up to 100 μM) of oleic acid and nucleotides, as indicated in the figure legends. Experiments were conducted in 25 mM Hepes (pH 7.0). Spectra were corrected by subtraction of their corresponding backgrounds. The molar ellipticity (deg cm^2 $dmol^{-1}$) is expressed as $[\theta]_h$ on a molar heme basis in the Soret and near-UV regions and as mean residue ellipticity $[\theta]_a$ in the far-UV region (mean residue relative molecular mass = 119 g/mol). Spectra were acquired with 0.5 nm/min resolution, and four scans were averaged per spectrum.

Analysis of the transition profile from native to the oleic acid-bound cyt *c* was performed according to a two-state model transition, assuming a linear dependence of the free energy change on the oleic acid concentration. Estimates of ΔG_0 (free energy of unfolding in the absence of oleic acid) and *C* (the oleic acid concentration required to produce half of the transition) were obtained as previously outlined (*22*). The same experiments were performed using GdnHCl (concentration range of 0−4 M) in place of oleic acid.

Peroxidase Activity Measurements. The peroxidase activity of cyt *c* (1 μM) and of the cyt *c*−oleic acid complex (at varying oleic acid concentrations) was measured using hydrogen peroxide and guaiacol (Sigma) in 25 mM Hepes at pH 7.0 and 25 °C. Product formation (tetraguaiacol; ε_{470} = 26.6 mM^{-1} cm^{-1}) was followed using a spectrophotometer. The concentrations were 10 mM guaiacol and 1 mM hydrogen peroxide. The same experiments were performed using GdnHCl (concentration range of 0−4 M) in place of oleic acid.

NMR Spectroscopy. The reference $^1H-^{15}N$ HSQC spectrum was collected for a sample containing 60 μM cyt *c* (ferric form of the wild type or the E62N mutant) in 25 mM Hepes (pH 7.0). Spectra were also recorded in the presence of ATP (3 or 30 mM, for both the wild type and the E62N mutant) or GTP (3 or 30 mM, for only the wild type). A spectrum was recorded upon addition of 30 mM ATP to wild-type cyt *c* in 100 mM phosphate buffer (pH 7.0).

Two-dimensional $^1H-^{15}N$ HSQC spectra were recorded at 25 °C on a Bruker Avance700 spectrometer equipped with a triple-resonance probe incorporating self-shielded gradient coils. A total of 2048 complex points in t_2 with 180 t_1 increments were acquired. The spectral widths were set to 11160 Hz in F_2 and 2270 Hz in F_1, positioning the carrier frequency at 4.70 ppm in F_2 and at 114.0 ppm in F_1. Quadrature detection in the indirectly detected dimensions was achieved using the States−TPPI method. Linear prediction and apodization 90°-shifted squared sine-bell functions were applied before Fourier transform. NMR data were processed and analyzed on Silicon Graphics workstations using NMRPipe and NMRView (*23, 24*). Chemical shift perturbation of NH groups upon addition of ATP or GTP was analyzed using the following index (*25*):

$$\Delta\delta_{HN} = \sqrt{\frac{(\Delta\delta_H{}^2 + \Delta\delta_N{}^2/25)}{2}}$$

where $\Delta\delta_H$ and $\Delta\delta_N$ are the differences in chemical shifts for amide H and N, respectively.

Cell-Free Extract Preparation. U937 cells (10^8) were suspended in 2 mL of lysis buffer at pH 7.4 (20 mM Hepes, 10 mM KCl, 1 mM EDTA, 1.5 mM $MgCl_2$, and 1 mM

EGTA), supplemented with a protease inhibitor cocktail (Sigma). After sitting on ice for 20 min, the cells were lysed in a Dounce homogenizer. The cell lysate was centrifuged at 2400*g* for 10 min at 4 °C, and the supernatant was further centrifuged at $10^5 g$ for 1 h. The resulting cytosolic fraction (S100) was used immediately or stored in aliquots at −80 °C. Extracts were quantitated by using the Bradford method (*26*).

Cell-Free Assays for Caspase Activity. The pro-apoptotic activity of wt cyt *c* and variants was assessed by their ability to activate caspases present in cytosolic extracts (S100). The S100 extract prepared from U937 cells (100 μg of proteins) was incubated for 1 h with 5 μM cyt *c* (wild type, R91N, E62N, K88E, and K88E/E62N), in lysis buffer and in the presence of 1 mM ATP at 25 °C. After incubation, 1 mM DTT and 25 μM *N*-acetyl-DEVD-AMC or *N*-acetyl-LEHD-AFC were added to measure the activity of caspase-3 and caspase-9, respectively. The caspase-3 activity of cell lysates in the presence of wt cyt *c* or E62N was assayed also via addition of different amounts of ATP or GTP. Hydrolysis of the substrate was followed fluorometrically at 380 nm (excitation) and 460 nm (emission) for the caspase-3 substrate AC-DEVD-AMC and at 400 and 505 nm for the caspase-9 substrate AC-LEHD-AFC.

Immunoblotting. Ten microliters of extracts (~10 μg of total proteins) was incubated for 1 h with 5 μM cyt *c* (wt, R91N, E62N, K88E, and K88E/E62N) in lysis buffer and in the presence of 1 mM ATP at 25 °C. After incubation, the samples were subjected to 10.5% SDS−PAGE and transferred to a nitrocellulose filter. Membrane was blocked overnight in 50 mM Tris (pH 8.0) containing 500 mM NaCl and 3% dried milk [blocking solution (BS)]; then it was probed for 3 h with anti-caspase-3 (rabbit polyclonal antibodies) in BS, followed by 1 h with the secondary IgG. The blots were visualized by "Kit chemiluminescent peroxidase substrate" (Sigma), according to the manufacturer's instructions.

RESULTS

Changes in cyt c Structure and Peroxidase Activity upon Binding to Oleic Acid. The structural characterization of oleic acid-bound cyt *c* and related mutants has been performed by CD. The far-UV CD spectra [200−250 nm (not shown)] of all the cytochrome *c* species investigated (wild type and mutants) are typical of proteins with an α-helix fold; they exhibit two negative Cotton effects at 208 and 222 nm of comparable strength. The Soret region CD spectra (400−450 nm, related to heme pocket structure) of wt cyt *c* and related mutants coincide with each other, all showing a positive and a negative Cotton effect at 408 and 416 nm, respectively. Changes induced by oleic acid in the heme crevice of proteins (monitored by following the gradual reduction of the 416 nm dichroic signal induced by increasing the concentration of oleic acid to 100 μM) are indicative of displacement of M80 from the axial coordination of the heme iron (*27, 28*). The fractions of oleic acid-induced species (*F*) and estimates of ΔG_0 (the free energy of unfolding in the absence of oleic acid) and *C* (the transition midpoint) were obtained as previously described (*19, 29*). For wt cyt *c*, the isothermal titration correlating *F* to the oleic acid concentration yields a sigmoidal curve (Figure 1A). The cyt *c* variants analyzed have curve profiles characterized by similar shapes and ΔG_0 values and do not display interactions with oleic acid significantly different from that of the wild type as indicated by the *C* values, with the exception of the K88E mutant (Table 1). As shown in Figure 1A, oleic acid induces a peroxidase activity increase in cyt *c* and mutants with an analogous sigmoidal dependence of the peroxidase activity on oleic acid concentration. Changes occurring in the tertiary structure of ferric cyt *c* once it binds to lipids imply the perturbation of the Fe−S(M80) bond and a partial protein unfolding. Such a rearrangement facilitates the access of small molecules, such as hydrogen peroxide, to the heme site, thus providing a reasonable explanation for the peroxidase activity shown by the oleic acid-bound protein. As for the CD results, the experimental data were fitted to a two-state model implying a conformational transition leading to a heme iron more accessible to peroxide. The fraction of protein bound to oleic acid showing peroxidase activity was evaluated from the absorbance value [*A*] at 470 nm and calculated as $F = ([A]_{obs} - [A]_0)/([A]_{ol} - [A]_0)$, where $[A]_{obs}$ is the absorbance measured at the various oleic acid concentrations and $[A]_0$ and $[A]_{ol}$ are the absorbance values at 0 and 100 μM fatty acid, respectively (i.e., the initial and oleic acid-induced final states, respectively) (Figure 1A). The curves obtained in the presence of oleic acid for wild-type cyt *c* and mutants describe a two-state transition similar to the curves obtained upon unfolding of cyt *c* by GdnHCl (Figure 1B) (*30*), although the free energy changes and the affinity values (*C*) obtained from fitting the transition measured by peroxidase activity are lower than those measured by the spectroscopic technique (Figure 1A,B and Table 1). These results suggest the existence of a low-free energy intermediate with peroxidase activity not evident in the CD measurements and point out that the partial unfolding of cyt *c* and mutant structures induced upon oleic acid binding yields modest but significant peroxidase activity

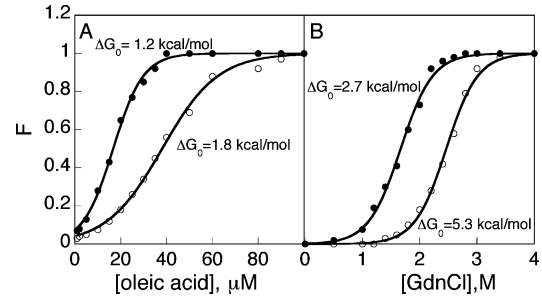

FIGURE 1: Comparison between unfolding and peroxidase activity increase induced by oleic acid and GdnHCl. Equilibrium unfolding of horse heart cyt *c* by oleic acid (A) and GdnHCl (B) at pH 7.0, plotted as best fits to a two-state transition model, followed by the increase in the molar ellipticity, $[\theta]_{416}$ (○), and peroxidase activity (●). For other details, see the text.

Table 1: *C* Values (micromolar) Determined for the Interaction of Oleic Acid with Wild-Type cyt *c* and Mutants, in the Absence or Presence of 3 mM ATP As Measured by CD Spectroscopy and Peroxidase Activity

	CD_{416}		peroxidase activity	
protein	no ATP	3 mM ATP	no ATP	3 mM ATP
cyt *c*	38 ± 3	53 ± 3	17 ± 2	25 ± 3
R91N	37 ± 2	36 ± 3	17 ± 2	17 ± 1
E62N	35 ± 2	34 ± 2	16 ± 2	14 ± 1
K88E	56 ± 5	52 ± 4	22 ± 2	22 ± 1
K88E/E62N	32 ± 1	31 ± 2	15 ± 3	16 ± 2

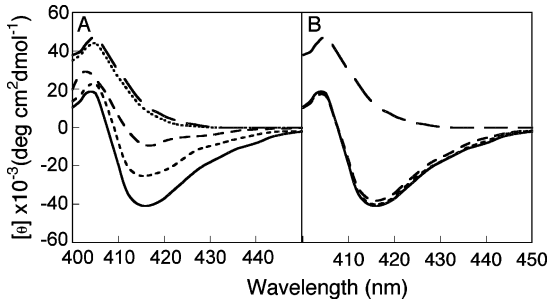

FIGURE 2: Effect of ATP and GTP on the structure of wt cyt *c* and the E62N mutant. Soret CD spectra of 7 μM cyt *c* alone (—) and in the presence of 100 μM oleic acid (— — —) and upon addition of ATP (---) or GTP (•••) at 3 (A) or 30 mM (B). Spectra of the E62N mutant (— — —) in the presence of 100 μM oleic acid and 3 (A) or 30 mM ATP (B) are shown, while the spectra of E62N alone and in the presence of 100 μM oleic acid are identical to the corresponding wt cyt *c* spectra. Soret CD spectra of K88E, R91N, and K88E/E62N are similar to the E62N spectra. Experiments were conducted in 25 mM Hepes (pH 7.0) at 25 °C. For other details, see the text.

values (140−170 nM s^{-1}). These values are 8−10 times lower when compared to the large increase measured upon complete cyt *c* unfolding in 4 M GdnHCl (i.e., 1400 nM s^{-1}).

Effects of ATP on the Structure and Peroxidase Activity of Oleic Acid-Bound cyt c. The addition of ATP induces no changes in the CD spectra of free (wt and mutated) cyt *c*, as previously reported (*11, 19*). Conversely, the addition of 3 mM ATP has relevant effects on the CD spectra of the wt cyt *c*−oleic acid complex with the recovery of the Soret negative band centered at 414 nm [with a blue shift with respect to the native cyt *c*, smaller than the one previously described at a higher oleic acid concentration (*19*)]. At variance, addition of 3 mM ATP brings about a significantly lower recovery of the Soret negative band in the spectra of E62N−, K88E−, R91N−, and K88E/E62N−oleic acid complexes (Figure 2A). Importantly, 3 mM GTP has no effect on the binding of oleic acid to wt cyt *c* or mutants (Figure 2A). As shown in Figure 2B, at 30 mM, both ATP and GTP fully dissociate the cyt *c*−oleic acid complexes here investigated.

Furthermore, addition of 3 mM ATP to oleic-bound cyt *c* significantly decreased the affinity of wt cyt *c* for oleic acid (as measured as the oleic acid concentration *C* required to produce half of the maximum CD spectral change at 416 nm or half of the maximum peroxidase activity). By contrast, the four mutant proteins exhibit *C* values in the presence of 3 mM ATP that can be considered similar, within standard error, to those measured in the absence of the nucleotide (Table 1).

Effect of ATP on cyt c Reduction by GSH. We examined the effect of ATP on the reduction induced by the physiological reductant GSH by analyzing the absorbance spectrum of cyt *c* in the 500−600 nm wavelength range. The absorbance at 550 nm (α-band) is characteristic of the reduced form and is not present in oxidized cyt *c*. As shown in Figure 3A, 1 mM GSH reduces the oxidized cyt *c* and 3 mM ATP slows the redox transition. The characteristic absorbance at 550 nm, continuously monitored to evaluate the redox potency of GSH on cyt *c*, shows a considerable decrease in the rate of reduction in the presence of 3 mM ATP (Figure 3B).

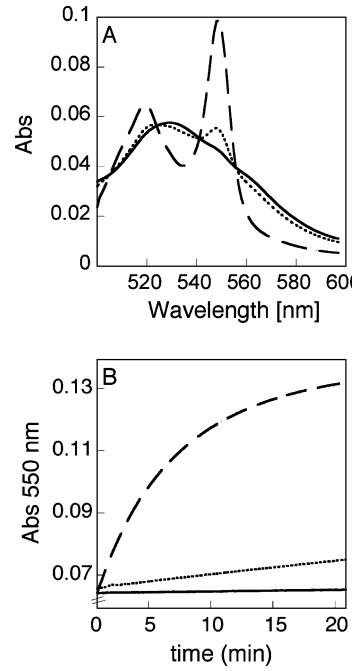

FIGURE 3: Effect of ATP on cyt *c* reduction by GSH. The effects of GSH and ATP on the redox state of cyt *c* were measured following (A) the spectral changes between 500 and 600 nm. The solid line shows the spectrum of oxidized cyt *c*, the dashed line the spectrum of reduced cyt *c* in the presence of GSH, and the dotted line the spectrum of cyt *c* treated with GSH and ATP. (B) The absorbances at 550 nm of oxidized cyt *c* (—), cyt *c* with GSH (— — —), and cyt *c* with GSH and ATP (•••) were continuously recorded.

NMR Studies of the ATP−cyt c Interaction. The interaction of ATP with wt cyt *c* and E62N has been investigated at a molecular level by NMR spectroscopy at pH 7.0. For this purpose, ^{15}N-labeled proteins were employed. We performed a chemical shift perturbation analysis of ^{1}H−^{15}N backbone amide groups following the chemical shift variations in the HSQC spectrum of wt cyt *c*, upon addition of 3 and 30 mM ATP or GTP in 25 mM Hepes buffer (pH 7.0). Furthermore, the interaction of the ^{15}N-labeled E62N mutant protein has been investigated in the presence of 3 and 30 mM ATP. The starting point was the acquisition of the ATP-free spectrum of cyt *c*, the assignment of which is already available (*31*). The pH value was accurately checked to ensure that resonance perturbations were due exclusively to ATP or GTP addition.

There are three phosphate-binding sites proposed for cyt *c* (*32*) (see Figure 4A for structural details). The first, and the best characterized, is formed by K88 and R91 (hereby called S1). The second and third proposed binding sites are located close to K25, H26, and K27 (S2) and at the heme crevice near K13 (S3), respectively (*32*). In a recent work, it was hypothesized that interaction of ATP with cyt *c* may involve E62 as part of the S1 site, with its side chain interacting with the nucleotide base (*19*).

Globally, addition of ATP in Hepes buffer causes chemical shift changes that are small and limited to a very reduced subset of residues on both wt and mutant protein as shown in Figure 4B,C. Residues exhibiting chemical shift changes are T89 of S1; V20, K22, G24, L32, and T102 of S2; and F82 of S3, beyond residue T47. Significantly, the largest variation observed is in the T89 chemical shift. When

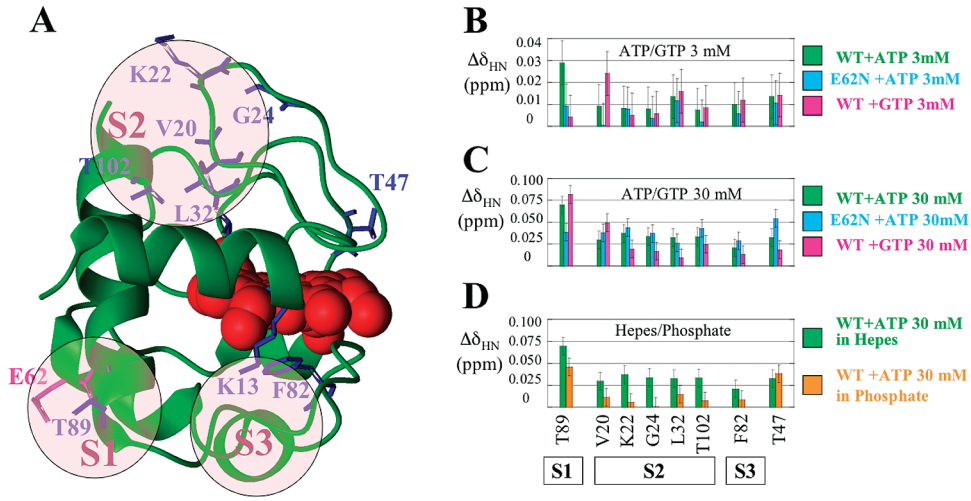

FIGURE 4: Interaction of ATP and GTP with wt cyt *c* and the E62N mutant. (A) Ribbon representation of cyt *c* showing as shaded areas the three nucleotide interaction sites, indicated as S1, S2, and S3. (B and C) NH chemical shift variation upon addition in 25 mM Hepes buffer of ATP to wt cyt *c* (green) and E62N (cyan) or upon addition of GTP to wt cyt *c* (magenta) at (B) 3 and (C) 30 mM added nucleotide. (D) NH chemical shift variation upon addition of ATP to wt cyt *c* in 25 mM Hepes (green) or in 100 mM phosphate buffer (orange). Only residues that show a significant perturbation are displayed.

compared to the chemical shift perturbation of other sites, the effect on S1 is much more pronounced at 3 mM than at 30 mM ATP. T89 chemical shift perturbation is significantly reduced for the E62N mutant at a low physiological ATP concentration (3 mM), supporting the hypothesis that E62 is important for binding of ATP to S1 (*19*). On the other hand, Figure 4C shows that at high ATP concentration (30 mM) all the above-mentioned residues show a clear perturbation, also for the E62N form, indicating that all three sites are affected. This result is in line with the observation that at high ATP concentrations the E62N mutant behaves in the same way as the wild type with regard to the ability of the nucleotide to interact with the protein. To further investigate the specific contribution made by the nucleoside moiety in the interaction of ATP with cyt *c*, we analyzed the effect of GTP on chemical shifts of wt cyt *c* at 3 mM (Figure 4B) and 30 mM (Figure 4C). Interaction of GTP with cyt *c* involves the same residues perturbed by ATP, but the chemical shift perturbation on T89 is again significantly reduced at low nucleotide concentrations, with residue V20 being the most perturbed (Figure 4B).

The slight overall perturbation upon addition of ATP indicates a weak interaction. To reduce the nonspecific effect of electrostatic forces, interaction of cyt *c* with ATP was investigated also in 100 mM phosphate buffer (Figure 4D). The negatively charged ATP molecule competes with buffer anions, which are in large excess and may mask the electrostatic contribution coming from the phosphate moiety of the nucleotide molecule. Also in phosphate buffer, addition of 30 mM ATP induces very small chemical shift differences, and again, the most perturbed residue is T89. Apart from T47, which is also significantly affected by addition of ATP in phosphate buffer, the other residues slightly perturbed by ATP in Hepes (V20, K22, G24, L32, F82, and T102) do not present appreciable chemical shift differences when ATP is added in phosphate buffer.

The lack of NH chemical shift perturbation for S2 and S3 can be explained by the stabilizing effect on cyt *c* of phosphate anions, which probably make direct interactions with all the three phosphate binding sites, protecting S2 and S3 from ATP perturbation. Phosphate stabilization is not sufficient for S1, suggesting a selective role in the interaction played by the base moiety in addition to the electrostatic component.

Incidentally, residue T47, which does not belong to any of the three sites, also displays a chemical shift perturbation. This result can be interpreted as an indirect structural consequence of ATP binding to the S1 site.

Caspase Activation in Cell-Free Systems. The apoptotic activity of cyt *c* variants has been compared with that of wt cyt *c* by using a cell-free activation assay. To rule out structural changes in the cyt *c* variants, their secondary and tertiary structures were checked by circular dichroism and electronic absorption spectral analysis. The variants show spectra identical to that of wt cyt *c*, thus suggesting the conservation of the proper folding and intactness of the cyt *c* variant structures (data not shown). As shown in Figure 5A, addition of exogenous 5 μM cyt *c* and 1 mM ATP to an in vitro system of cytosolic fractions from U937 cells induces caspase activation, as measured by using the caspase-3-specific Ac-DEVD-AMC and the caspase-9-specific Ac-LEHD-AFC fluorogenic substrates. Among the cyt *c* variants, the K88E mutant is the only one showing potency comparable to that of the wt protein, while the other mutants show lower activity. For all proteins, the cleavage of caspase-9 substrate occurs to a minor extent versus that of the caspase-3 substrate. Furthermore, the effect of ATP binding to the S1 site for the pro-apoptotic activity of cyt *c* was assayed in the presence of an increasing amount of ATP or GTP (Figure 5B). With respect to wt cyt *c*, the highest caspase-3 activity values are in the ATP concentration range from 1 to 3 mM, while the same concentrations of GTP are much less effective. Higher concentrations of ATP (5−10 mM) inhibit the caspase activity. On the other hand, when the ATP concentrations exerting the strongest effect on the wt cyt *c* apoptotic activity are used in the E62N mutant assays, caspase-3 activities appear to be much lower. The caspase-3 activation, as indicated by DEVDase activity measurement, was confirmed by Western blot detection of procaspase-3 cleavage and by densitometric analysis (Figure 5C,D).

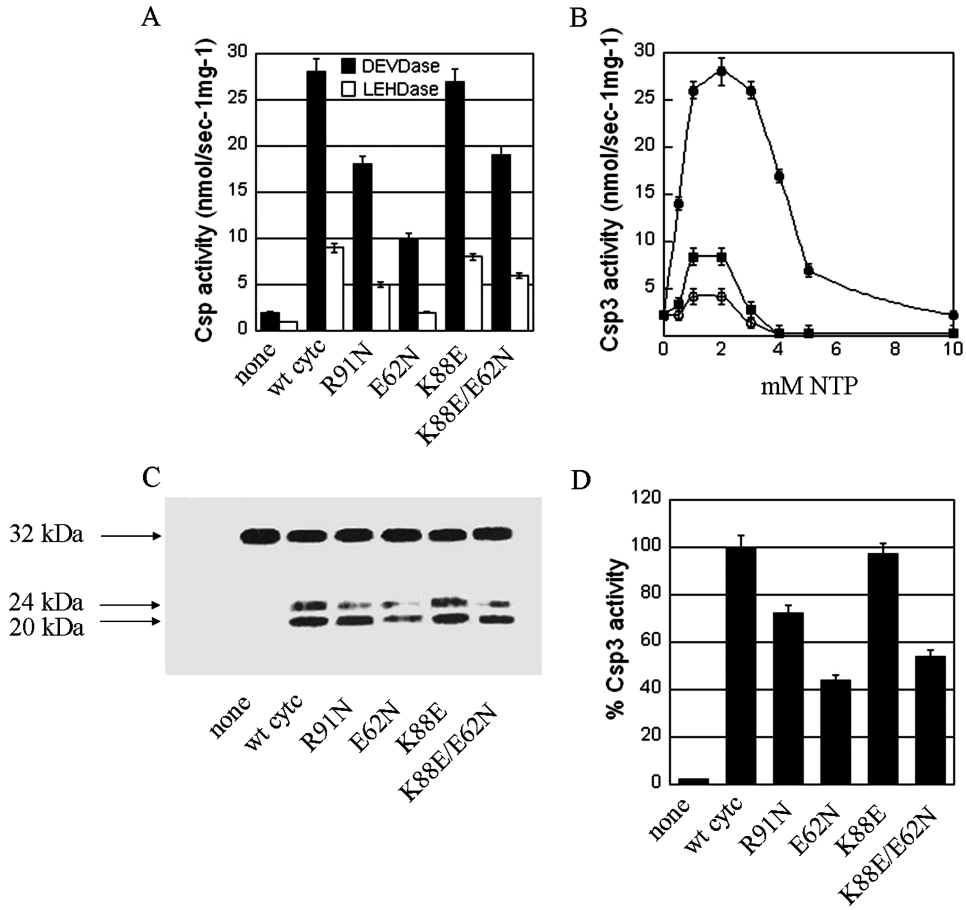

FIGURE 5: Pro-apoptotic activity of wt cyt *c* and mutants. (A) Caspase-3 and caspase-9 activities of fresh U937 cytosol (100 μg) incubated with wt cyt *c* (5 μM) as control or R91N, E62N, K88E, and K88E/E62N variants (5 μM) in the presence of 1 mM ATP for 1 h at 25 °C were measured fluorometrically by hydrolysis of the substrates DEVD-AMC and LEHD-AFC, respectively. (B) Caspase-3 activity was measured with wt cyt *c* (5 μM) in the presence of increasing concentrations of ATP (●) or GTP (○) and E62N (5 μM) in the presence of increasing concentrations of ATP (■). (C) Processing of pro-caspase-3 was assessed by incubating fresh U937 cytosol (10 μg) with wt cyt *c* (5 μM) as a control or R91N, E62N, K88E, and K88E/E62N variants (5 μM) in the presence of 1 mM ATP for 1 h at 25 °C and analyzed by Western blotting. (D) The amount of processed caspase-3 was quantified by densitometric analysis and expressed as a percentage of control to which a value of 100 has been given. Results are means ± the standard deviation of triplicate experiments.

DISCUSSION

The unfolding of horse heart cyt *c* (wt and variants) has been observed by the reduction of the magnitude of the CD signal at 416 nm and by the increase in the peroxidase activity. By using as denaturants both GdnHCl and oleic acid, the experimental data show a sigmoidal dependence on denaturant concentration and are fitted by a two-state model of unfolding (*19, 30, 33*). Previous studies have shown that nonesterified fatty acids, phospholipid vesicles, and SDS monomers and micelles induce in cyt *c* conformational changes related to the formation of a compact state possessing nativelike secondary structure but fluctuating tertiary conformation. These changes involve the heme pocket region and in particular determine the weakening of the M80−Fe(III) axial bond (*19, 34*−*36*), an event known to precede the global unfolding of *c*-type cytochromes (*37*−*40*). Such partial unfolding of cyt *c* in the presence of cardiolipin liposomes has been suggested to be responsible for the induction of peroxidase activity (*6, 7*). In agreement with these findings, in this study a peroxidase activity increase was observed in the presence of oleic acid, accompanied by a conformational transition characterized by an apparent free energy change smaller than that measured by CD spectroscopy. Curve profiles similar to those observed in the presence of GdnHCl were observed, but in this latter case, the free energy change values are sensibly higher than those measured in the presence of oleic acid. Furthermore, the data indicate that the measurement of peroxidase activity, which is necessarily related to an increased accessibility of the heme iron, allows to detect an unfolding transition with a lower free energy with respect to the transition induced by the loss of M80−Fe(III) coordination. Such a sensitivity of the peroxidase assay in detecting small amounts of "partially" unfolded species at low concentrations of oleic acid is further suggested by the lower transition midpoints, *C*, for peroxidase activity as compared to the CD_{416} measurements. In the case of the K88E mutant, higher *C* values indicate a weaker binding of oleic acid to this variant with respect to wt cyt *c*. Conversely, the E62N, R91N, and E62N/K88E mutants display affinities comparable to that of the wt protein.

Studies on cyt *c*−phospholipid interactions indicated the presence of at least two different lipid-binding sites on the protein, named the A-site and the C-site (*41*). The A-site is a high-affinity site thought to be composed of a network of basic residues, including K72, K73, and K86, which electrostatically interact with the deprotonated form of negatively charged lipids. Weaker binding of oleic acid to the K88E cyt *c* variant points to the involvement of K88 in building

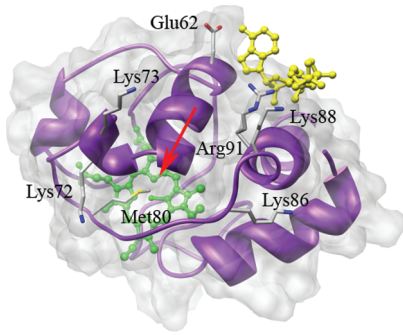

FIGURE 6: Schematic representation of the three-dimensional structure of the ATP−cyt *c* complex obtained by docking simulations. ATP binding residues E62, K88, and R91 and residues building up the A-site for charged lipid binding (K72, K73, and K86) are shown in stick representation together with the heme ligand M80. Heme and ATP are shown in ball-and-stick representation and colored green and yellow, respectively. The red arrow indicates the approximate location of the hydrophobic pocket giving direct access to the heme cavity on the M80 side.

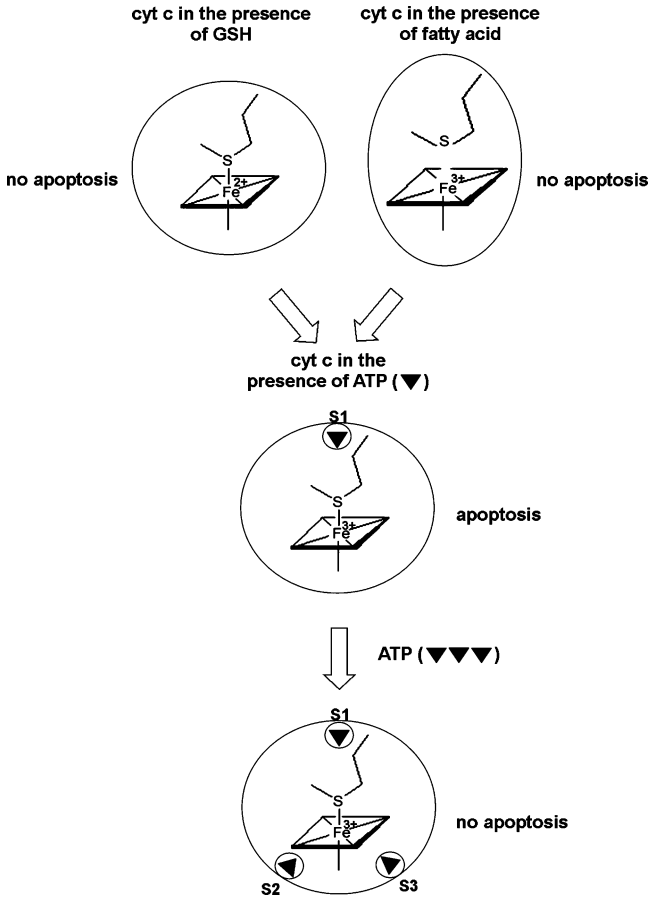

FIGURE 7: Schematic overview of the effects of ATP binding to cyt *c*. ATP at a low millimolar concentration binds to cyt *c* site S1 and drives structural transitions among different conformations and/or different redox status of the protein to bring about cell apoptosis. ATP at higher concentrations binds also to S2 and S3 sites and inhibits apoptosis.

up the above-mentioned charge network. In addition, K88 is located in the same protein region of K72, K73, and K86, and these four lysine residues are located on the rim of a pocket on the cyt *c* surface, which gives direct access to the heme cavity on the M80 side (Figure 6). With the aim of comparing the effect of ATP on the binding of oleic acid to the ferric forms of wt cyt *c* and mutants, we determined the transition midpoints, *C*, in the presence of 3 mM ATP. Indeed, ATP (and not GTP) significantly decreased the affinity of wt cyt *c* for oleic acid, while it had no effect on any of the mutants. It might be argued that ATP competes with oleic acid for the same binding site on cyt *c*. Such a possibility is consistent with our previous results that, on the basis of docking simulations (*19*), suggested a role for residues K88 and E62, in addition to the previously reported R91 (*11, 32, 42*), in the binding of ATP to cyt *c* (Figure 6) and demonstrated the capability of ATP to revert non-native states of cyt *c* back to the native conformation. By site-directed mutagenesis experiments, we now definitely demonstrate that in horse cyt *c* residues E62, K88, and R91 are involved in ATP-specific binding at low millimolar concentrations. Importantly, the concentration range of ATP present in the cytoplasm of living cells is 1−10 mM (*43, 44*), sufficient for binding to cyt *c* (*32*) and approximately one order of magnitude higher than that of GTP, which is estimated to be 0.3−0.6 mM (*45*). Some authors stated that, in the cyt *c*−ATP interaction, two low-affinity sites and one higher-affinity site for the nucleotide exist on the protein, and they proposed for the high-affinity site a regulatory role in the respiratory chain (*32*). The NMR results presented here indicate that the ATP binding to the site here named S1 (containing K88 and R91 residues with E62) brings about the largest structural perturbation, as judged by the magnitude of chemical shift variation. Such an effect is reduced by mutation of E62. On the other hand, this effect persists in 100 mM phosphate buffer, when anions at a high concentration presumably interact with the basic surface of this protein. The S1 site is the only of the three phosphate binding sites that still shows a clear perturbation upon addition of ATP. A high concentration of this nucleotide is not able to induce significant changes in S2 and S3, where the electrostatic interaction with phosphate ions prevents a significant perturbation by ATP. Interestingly, unlike ATP, GTP mostly perturbs the S2 site. On the basis of these data, we proposed a further regulatory role for the ATP−S1 interaction; such binding may in fact induce in the protein structural transitions (and/or stabilize conformations), which facilitate the interaction with physiological partners (such as Apaf-1 in the apoptotic machinery). Indeed, the binding of cyt *c* to Apaf-1 involves many residues located in different areas of the surface, particularly lysine residues located around the heme edge (K7, K25, K39, and K72) that interact with the negatively charged aspartate residues in the Apaf-1 WD-40 domain (*17, 18*). Such residues do not appear to be involved in ATP binding at low millimolar concentrations. Recent evidence demonstrates that ATP (5−10 mM) completely blocks apoptosome formation by binding to cyt *c* and preventing cyt *c*−Apaf-1 interaction (*44, 46*). NMR results also confirm that at high concentrations, ATP (and GTP) does not discriminate among the three sites located on different areas of the cyt *c* surface; this is true for wt cyt *c* and the E62N mutant, which exhibit similar interaction profiles.

We have therefore probed the effect of mutations in the S1 site on cyt *c* pro-apoptotic activity using the cell-free apoptosis system described in previous reports (ref *47* and references cited therein). Cyt *c* can initiate caspase activation in an in vitro reconstitution system containing cyt *c*, Apaf-1, ATP, procaspase-9, and procaspase-3. Significantly, our results show that the maximum pro-apoptotic activity of cyt

c occurs in the presence of ATP at concentrations ranging from 1 to 3 mM. At higher concentrations (5−10 mM), ATP shows the inhibitory effect discussed above. GTP, which mostly perturbs the S2 site with respect to the S1 site, seems to be much less effective. The decreased E62N mutant apoptotic potency may be explained on the basis of the reduced level of binding of ATP to such a cyt *c* variant, accordingly to the importance of the S1 site for the apoptotic activity of cyt *c*.

It has been reported that cyt *c* released from the mitochondria as holoprotein with its prosthetic group will almost certainly be in the oxidized state (*48*). According to previously published results (*49*), we observed that oxidized cyt *c* was quickly reduced upon addition to cytosolic extracts (data not shown). The finding that ferric cyt *c* (and not ferrous cyt *c*) is the caspase activator in the cytosol (*14*−*16, 50*) suggests that cyt *c* with oxidized heme is in the conformation capable of interacting with Apaf-1 and forming the apoptosome. When cyt *c* is in the presence of GSH, a reductant present in the cell cytoplasm, its spectrum shows the α-band at 550 nm characteristic of ferrous cyt *c*. The addition of ATP brings about a significant decrease in the magnitude of this band and slows cyt *c* reduction. This is consistent with the view reported by other authors on the ATP binding to the R91-containing site in the oxidized form of the protein (*51*) and with the present suggestion for the role of such binding in regulating the rate of reduction of cyt *c*, thus promoting apoptosis in the cytosol. Recently, the ability of the reduced environment of cells treated with GSH to inhibit cyt *c*-mediated apoptosis as a result of the specific inactivation of cyt *c* has been suggested (*52*). On the basis of our evidence that mutations of the R91 and E62 residues indeed reduce the apoptotic activity of cyt *c*, here we propose that at low millimolar concentrations, the binding of ATP to the S1 site stabilizes cyt *c* in the suitable conformation for the interaction with Apaf-1 and activation of the caspase cascade. In this regard, the negligible effect of the K88 mutation on the apoptotic activity of cyt *c* may be explained considering that other basic residues surrounding K88 (e.g., K86, K87, and R91) may replace this residue in the ATP attachment site.

In summary, the previous statements about the ATP requirement for apoptosome activation at low millimolar concentrations (*53*) and the inhibition of apoptosome formation by ATP at high concentrations (*45, 47*) well correlate with the results of this study, which provide for ATP binding on the cyt *c* S1 site in the cytosol a novel regulatory role in apoptosis (Figure 7), in addition to the well-known role in the oxidative phoshorylation in mitochondria (*1*).

ACKNOWLEDGMENT

We thank Dr. Monica Bari for providing U937 cells and Prof. Massimiliano Coletta for helpful discussion.

REFERENCES

1. Craig, D. B., and Wallace, C. J. (1995) Studies of 8-azido-ATP adducts reveal two mechanisms by which ATP binding to cytochrome c could inhibit respiration. *Biochemistry 34*, 2686–2693.
2. Touminem, E. K., Wallace, C. J., and Kinnunen, P. K. (2002) Phospholipid-cytochrome *c* interaction: Evidence for the extended lipid anchorage. *J. Biol. Chem. 277*, 8822–8826.
3. Stewart, J. M., Blakely, J. A., and Johnson, M. D. 200 The interaction of ferrocytochrome c with long-chain fatty acids and their CoA and carnitine esters. *Biochem. Cell Biol. 78*, 675–681.
4. Zucchi, M. R., Nascimento, O. R., Faljoni-Alario, A., Pietro, T., and Nantes, I. L. (2003) Modulation of cytochrome c spin states by lipid acyl chains: A continuous-wave electron paramagnetic resonance (CW-EPR) study of haem iron. *Biochem. J. 370*, 671–678.
5. Sinibaldi, F., Fiorucci, L., Patriarca, A., Lauceri, R., Ferri, T., Coletta, M., and Santucci, R. (2008) Insights into cytochrome c-cardiolipin interaction. Role played by ionic strength. *Biochemistry 47*, 6928–6935.
6. Belikova, N. A., Vladimirov, Y. A., Osipov, A. N., Kapralov, A. A., Tyurin, V. A., Potapovich, M. V., Basova, L. V., Peterson, J., Kurnikov, I. V., and Kagan, V. E. (2006) Peroxidase activity and structural transitions of cytochrome c bound to cardiolipin-containing membranes. *Biochemistry 45*, 4998–5009.
7. Kapralov, A. A., Kumikov, I. V., Vlasova, I. I., Belikova, N. A., Tyurin, V. A., Basova, L. V., Zhao, Q., Tyurina, Y. Y., Jiang, J., Bayer, H., Vladimirov, Y. A., and Kagan, V. E. (2007) The hierarchy of structural transitions induced in cytochrome c by anionic phospholipids determines its peroxidise activation and selective peroxidation during apoptosis in cells. *Biochemistry 46*, 14232–14244.
8. Kawai, C., Prado, F. M., Nunes, G. L. C., Di Mascio, P., Carmona-Rebeiro, A. M., and Nantes, I. L. (2005) pH-dependent interaction of cytochrome c with mitochondrial mimetic membranes: The role of an array of positively charged amino acids. *J. Biol. Chem. 280*, 34709–34717.
9. Gorbenko, G. P., Molotkovsky, J. G., and Kinnunen, P. K. (2006) Cytochrome C interaction with cardiolipin/phosphatidylcholine model membranes: Effect of cardiolipin protonation. *Biophys. J. 90*, 4093–4103.
10. Kalanxhi, E., and Wallace, C. J. (2007) Cytochrome c impaled: Investigation of the extended lipid anchorage of a soluble protein to mitochondrial membrane models. *Biochem. J. 407*, 179–187.
11. Tuominen, E. K. J., Zhu, K., Wallace, C. J. A., Clark-Lewis, I., Craig, D. B., Rytomaa, M., and Kinnunen, P. K. J. (2001) ATP induces a conformational change in lipid-bound cytochrome c. *J. Biol. Chem. 276*, 19356–19362.
12. Ott, M., Zhivotovsky, B., and Orrenius, S. (2007) Role of cardiolipin in cytochrome c release from mitochondria. *Cell Death Differ. 14*, 1243–1247.
13. Green, D. R., and Redd, J. C. (1998) Mitochondria and apoptosis. *Science 281*, 1309–1312.
14. Pan, Z., Voehringer, D. W., and Meyn, R. E. (1999) Analysis of redox regulation of cytochrome c-induced apoptosis in a cell-free system. *Cell Death Differ. 6*, 683–688.
15. Suto, D., Sato, K., Ohba, Y., Yoshimura, T., and Fujii, J. (2005) Suppression of the pro-apoptotic function of cytochrome c by singlet oxygen via a haem redox state-independent mechanism. *Biochem. J. 392*, 399–406.
16. Brown, G. C., and Borutaite, V. (2008) Regulation of apoptosis by the redox state of cytochrome c. *Biochim. Biophys. Acta 1777*, 877–881.
17. Purring-Koch, C., and McLendon, G. (2000) Cytochrome c binding to Apaf-1: The effects of dATP and ionic strength. *Proc. Natl. Acad. Sci. U.S.A. 97*, 11928–11931.
18. Yu, T., Wang, X., Purring-Kock, C., Wie, Y., and McLendon, G. (2001) A mutational epitope for cytochrome C binding to the apoptosis protease activation factor-1. *J. Biol. Chem. 276*, 13034–13038.
19. Sinibaldi, F., Mei, G., Polticelli, F., Piro, M. C., Howes, B. D., Smulevich, G., Santucci, R., Ascoli, F., and Fiorucci, L. (2005) ATP specifically drives refolding of non-native conformations of cytochrome c. *Protein Sci. 14*, 1049–1058.
20. Patel, N. C., Lind, M. C., and Pielak, G. J. (2001) Characterization of horse cytochrome c expressed in *Escherichia coli*. *Protein Expression Purif. 22*, 220–224.
21. Sinibaldi, F., Hower, B. D., Smulevich, G., Ciaccio, C., Coletta, M., and Sntucci, R. (2003) Anion concentration modulates the conformation and stability of the molten globule of cytochrome c. *JBIC, J. Biol. Inorg. Chem. 8*, 663–670.
22. Knapp, J. A., and Pace, C. N. (1974) Guanidine hydrochloride and acid denaturation of horse, cow, and *Candida krusei* cytochromes c. *Biochemistry 13*, 1289–1294.
23. Delaglio, F., Grzesiek, S., Vuister, G. W., Zhu, G., Pfeifer, J., and Bax, A. (1995) NMRPipe: A multidimensional spectral processing system based on UNIX pipes. *J. Biomol. NMR 6*, 277–293.

24. Johnson, B. A. (2004) Using NMRView to visualize and analyze the NMR spectra of macromolecules. *Methods Mol. Biol. 278*, 313–352.
25. Grzesiek, S., Stahl, S. J., Wingfield, P. T., and Bax, A. (1996) The CD4 determinant for down-regulation by HIV-1 Nef directly binds to Nef. Mapping of the Nef binding surface by NMR. *Biochemistry 35*, 10256–10261.
26. Bradford, M. M. (1976) A rapid and sensitive method for the quantitation of microgram quantities of protein utilizing the principle of protein-dye binding. *Anal. Biochem. 72*, 248–254.
27. Pielak, G. J., Oikawa, K., Mauk, A. G., Smith, M., and Kay, C. M. (1986) Elimination of the negative Soret Cotton effect of eukaryotic cytochrome c by replacement of an invariant phenylalaline residue by site-directed mutagenesis. *J. Am. Chem. Soc. 108*, 2724–2727.
28. Santucci, R., and Ascoli, F. (1997) The Soret circular dichroism spectrum as a probe for the heme Fe(III)-Met(80) axial bond in horse cytochrome c. *J. Inorg. Biochem. 68*, 211–214.
29. Agueci, F., Polticelli, F., Sinibaldi, F., Piro, M. C., Santucci, R., and Fiorucci, L. (2007) Probing the effect of mutations on cytochrome C stability. *Protein Pept. Lett. 14*, 335–339.
30. Diederix, R. E., Ubbink, M., and Canters, G. W. (2002) Peroxidase activity as a tool for studying the folding of c-type cytochromes. *Biochemistry 41*, 13067–13077.
31. Liu, W., Rumbley, J., Englander, S. W., and Wand, A. J. (2003) Backbone and side-chain heteronuclear resonance assignments and hyperfine NMR shifts in horse cytochrome c. *Protein Sci. 12*, 2104–2108.
32. Craig, D. B., and Wallace, C. J. (1991) The specificity and Kd at physiological ionic strength of an ATP-binding site on cytochrome c suit it to a regulatory role. *Biochem. J. 279*, 781–786.
33. Santoro, M. M., and Bolen, D. W. (1992) A test of the linear extrapolation of unfolding free energy changes over an extended denaturant concentration range. *Biochemistry 31*, 4901–4907.
34. Hildebrandt, P., Heimburg, T., and Marsh, D. (1990) Quantitative conformational analysis of cytochrome c bound to phospholipid vesicles studied by resonance Raman spectroscopy. *Eur. Biophys. J. 18*, 193–201.
35. Dopner, S., Hildebrandt, P., Rosell, F. I., Mauk, A. G., Von Walter, M., Buse, G., and Soulimane, T. (1999) The structural and functional role of lysine residues in the binding domain of cytochrome c in the electron transfer to cytochrome c oxidase. *Eur. J. Biochem. 261*, 379–391.
36. Oellerich, S., Wackerbarth, H., and Hildebrandt, P. (2003) Conformational equilibria and dynamics of cytochrome c induced by binding of sodium dodecyl sulfate monomers and micelles. *Eur. Biophys. J. 32*, 599–613.
37. Sinibaldi, F., Piro, M. C., Howes, B. D., Smulevich, G., Ascoli, F., and Santucci, R. (2003) Rupture of the hydrogen bond linking two Omega-loops induces the molten globule state at neutral pH in cytochrome c. *Biochemistry 42*, 7604–7610.
38. Godbole, S., Dong, A., Garbin, K., and Bowler, B. E. (1997) A lysine 73 → histidine variant of yeast-1-cytochrome c: Evidence for a native-like intermediate in the unfolding pathway and implications for m value effects. *Biochemistry 36*, 119–126.
39. Krishna, M. M., Maity, H., Rumbley, J. N., Lin, Y., and Englander, S. W. (2006) Order of steps in the cytochrome C folding pathway: Evidence for a sequential stabilization mechanism. *J. Mol. Biol. 359*, 1410–1419.
40. Balakrishnan, G., Hu, Y., Oyerinde, O. F., Su, J., Groves, J. T., and Spiro, T. G. (2007) A conformational switch to β-sheet structure in cytochrome c leads to heme exposure. Implications for cardiolipin peroxidation and apoptosis. *J. Am. Chem. Soc. 129*, 504–505.
41. Rytomaa, M., and Kinnunen, P. K. J. (1995) Reversibility of the binding of cytochrome c to liposomes. Implications for lipid-protein interactions. *J. Biol. Chem. 270*, 3197–3202.
42. Craig, D. B., and Wallace, C. J. (1995) Studies of 8-azido-ATP adducts reveal two mechanisms by which ATP binding to cytochrome c could inhibit respiration. *Biochemistry 34*, 2686–2693.
43. Skoog, L., and Bjursell, G. (1974) Nuclear and cytoplasmic pools of deoxyribonucleoside triphosphates in Chinese hamster ovary cells. *J. Biol. Chem. 25*, 6434–6438.
44. Chandra, D., Bratton, S. B., Person, M. D., Tian, Y., Martin, A. G., Ayres, M., Fearnhead, H. O., Gandhi, V., and Tang, D. G. (2006) Intracellular nucleotides act as critical prosurvival factors by binding to cytochrome C and inhibiting apoptosome. *Cell 125*, 1333–1346.
45. Hatakeyama, K., Harada, T., and Kagamiyama, H. (1992) IMP dehydrogenase inhibitors reduce intracellular tetrahydrobiopterin levels through reduction of intracellular GTP levels. Indications of the regulation of GTP cyclohydrolase I activity by restriction of GTP vailability in the cells. *J. Biol. Chem. 267*, 20734–29739.
46. Samali, A., O'Mahoney, M., Reeve, J., Logue, S., Szegezdi, E., McMahon, J., and Fearnhead, H. O. (2007) Identification of an inhibitor of caspase activation from heart extracts: ATP blocks apoptosome formation. *Apoptosis 12*, 465–474.
47. Deanault, J. B., and Salvesen, G. S. (2008) Apoptotic caspase activation and activity. *Methods Mol. Biol. 414*, 191–220.
48. Hancock, J. T., Desikan, R., and Neill, S. J. (2001) Does the redox status of cytochrome C act as a fail-safe mechanism in the regulation of programmed cell death? *Free Radical Biol. Med. 31*, 697–703.
49. Hampton, M. B., Fadeel, B., and Orrenius, S. (1998) Redox regulation of the caspases during apoptosis. *Ann. N.Y. Acad. Sci. 854*, 328–335.
50. Ghafourifar, P., Schenk, U., Klein, S. D., and Richter, C. (1999) Mitochondrial nitric-oxide synthase stimulation causes cytochrome c release from isolated mitochondria. Evidence for intramitochondrial peroxynitrite formation. *J. Biol. Chem. 274*, 31185–31188.
51. Corthesy, B. E., and Wallace, C. J. (1988) The oxidation-state-dependent ATP-binding site of cytochrome c. Implication of an essential arginine residue and the effect of occupancy on the oxidation-reduction potential. *Biochem. J. 252*, 349–355.
52. Vaughn, A. E., and Deshmukh, M. (2008) Glucose metabolism inhibits apoptosis in neurons and cancer cells by redox inactivation of cytochrome c. *Nat. Cell Biol. 10*, 1477–1483.
53. Genini, D., Budihardjo, I., Plunkett, W., Wang, X., Carrera, C. J., Cottam, H. B., Carson, D. A., and Leoni, L. M. (2000) Nucleotide requirements for the in vitro activation of the apoptosis protein-activating factor-1-mediated caspase pathway. *J. Biol. Chem. 275*, 29–34.

BI801837E